

High-resolution X-ray microdiffraction analysis of natural teeth

Jing Xue, Linling Zhang, Ling Zou, Yunmao Liao, Jiyao Li, Liying Xiao and Wei Li*

Received 27 May 2007

Accepted 31 January 2008

State Key Laboratory of Oral Diseases, Sichuan University, People's Republic of China.

E-mail: leewei2000@sina.com

The main component of natural teeth was determined many years ago as calcium phosphate, mostly in the form of hydroxyapatite with different crystallites. In the past, the method used in tooth crystal investigation has been mainly powder X-ray diffraction analysis, but this method has its drawbacks, *i.e.* the destruction of the natural tooth structure and the difficulty in examining the preferred orientation in different layers of the tooth. During the last century, microzone X-ray diffraction on the tooth surface was carried out, but, as the technology was less sophisticated, the results obtained were not very detailed. The newly developed microdiffraction equipment permits analysis of the microzone of teeth *in situ*. To test this new microdiffraction equipment, microdiffraction analysis of one natural healthy deciduous molar tooth and one carious deciduous molar tooth has been performed, using a Bruker D8 instrument. Phase analysis of the two teeth was performed; the crystal size at six test points in the natural healthy tooth was calculated by reflection (211), and the crystal preferred orientation of reflection (300) and reflection (002) at six test points in the natural healthy tooth were compared. The results showed that the tooth was a kind of biological mixed crystal composed of several crystal phases, the main crystal phase being hydroxyapatite. The crystal size grew larger going from the dentin to the enamel. The crystal preferred orientation mainly existed in the enamel, especially in the reflection (002). From our experiment, layer orientation and continuous crystal variations in teeth could be conveniently studied using fast online measurements by high-resolution X-ray microdiffraction equipment.

© 2008 International Union of Crystallography
Printed in Singapore – all rights reserved

Keywords: X-ray microdiffraction; enamel; caries; texture; crystal.

1. Introduction

The main mineral component of natural teeth was determined as calcium phosphate many years ago (Gross, 1926). Most of the calcium phosphate exists in the form of hydroxyapatite with different crystallites. In the initial stages of tooth decay, the hydroxyapatite crystallite changes and decomposes and, as a result, tooth decalcification occurs (Legeros, 1981, 1990; Featherstone *et al.*, 1978; Robinson *et al.*, 2000). Understanding the early variation in hydroxyapatite crystallite of natural teeth with caries is very important for both caries prevention mechanisms and the design of caries preventative agents. Based on the knowledge of hydroxyapatite chemistry, decalcification of teeth in the initial stages of decay may be associated with certain crystal variations and this process may be reversible (Legeros, 1999). Making use of X-ray diffraction (XRD) to analyse the process of caries progression will give us a greater understanding of the initial changes in the tooth and hence provide new ideas for caries prevention.

From powder X-ray diffraction patterns of a tooth, we are easily able to analyse the constituent phases of the tooth, crystallinity and

average crystallite size. However, this method requires that the tooth sample is ground into powder of a particular size, leading to destruction of the tooth structure. It is also very difficult to analyse a small zone affected by caries because the amount of powder obtained from the small zone will be insufficient for the diffraction method; also, the *in situ* crystal orientation is demolished after grinding. During the last century, microzone X-ray diffraction was carried out by some researchers, but, as the equipment was less sophisticated at that time, it was difficult to focus the X-ray beam on a small target area in a natural tooth with initial caries, the signal detected was very weak, and, as a result, the data obtained were not good enough for thorough analysis (Bergman & Lind, 1966). The recent developments of a new kind of high-resolution detector and the monocrystalline confocal lens have greatly improved the sensitivity of X-ray diffraction, and made it possible to analyse *in situ* the microzone of tooth mineral crystallite (Busson *et al.*, 1999; Friedel *et al.*, 2005; Nakano *et al.*, 2002). In order to test the usefulness of this technique in research into mineral crystal changes in normal and carious teeth, we carried out X-ray microdiffraction analysis of a natural tooth using high-resolution XRD equipped with GADDS (general area-detector

diffraction solution). It was hoped that X-ray diffraction of a small zone of tooth would reveal valuable and detailed data on tooth mineral structure in both healthy and carious teeth.

2. Materials and methods

2.1. Sample preparation

One natural healthy deciduous molar tooth and one carious deciduous molar tooth were obtained from patients undergoing extraction for severe periodontal disease, with informed consent. The two teeth were rinsed in distilled water, dried and sectioned into slices with a thickness of 3 mm so that they could easily be mounted on the XRD sample holder. The measuring points on the healthy tooth were determined along a line from the dentin to enamel surface by laser pointer and microscope originally equipped on the XRD. A total of eight points were employed in the analysis: six on the healthy tooth and two on the carious tooth (one inside the cavity and one outside the cavity).

2.2. XRD instrument

The X-ray microdiffraction instrument used for the analysis was a Bruker D8 DISCOVER with GADDS (Bruker, Karlsruhe, Germany). The instrument was equipped with a two-dimensional detector (HI-STAR, Bruker, Karlsruhe, Germany) and monocapillary lens with 50 μm and 100 μm microzone in diameter. The detection parameters of the instrument were as follows: Bruker D8 DISCOVER with GADDS, Cu $K\alpha$ radiation working at 40 kV and 40 mA, parallel graphite monochromator, monocapillary with a radius of 50 μm , 150 mm HI-STAR two-dimensional detector, scanning angle 8–102°, step size 0.02°, scan step time 1800 s.

The radius of the monocapillary lens was 50 μm , allowing us to examine layer orientation and continued decay variations in the tooth apatite crystal in a microzone.

2.3. Analysis

After the instruments were adjusted and set, the samples were mounted and fixed on the sample holders; a laser beam marked the focal point on the samples mounted in a quarter-circle Eulerian cradle on an xyz stage and the analysis spots were determined using the video microscope. The positions of the measuring points were determined (shown in Figs. 1A, 1B and 1C). Then the monocapillary optic focused the radiation exiting the fine-focus X-ray tube to the measuring point. The θ and 2θ angles were set from 8° to 102°. After the samples were measured by XRD, the data obtained were analysed using Bruker *DIFFRAC* plus the *EVA* program (AXS, Bruker, Karlsruhe, Germany), the reference database was the JCPDS card (Joint Committee on Powder Diffraction), the computer reference database was the ICDD PDF2/PDF4 reference database.

3. Results

3.1. X-ray diffractogram

The X-ray diffraction Debye ring patterns and diffractogram of the healthy tooth are shown in Figs. 2(A)–2(G), and of the carious tooth in Figs. 3(A)–3(C). In the healthy tooth the Debye ring patterns show that two points in the dentin and one at the enamel–dentin junction (EDJ) were intact and continuous, but the borderlines of rings were in definite, and some rings were mixed together, indicating that the crystallinity of the dentin was poor and there was no evident texture or crystal preferred orientation in the dentin. The other three points

in the enamel showed that the Debye rings were not intact and were discontinuous, the borderlines of rings were distinct, each ring could be separated from the others, indicating that the crystallinity of the enamel was better than that of dentin, and that crystal preferred orientation existed in the enamel. The diffractogram of six points shown in Fig. 2(G) also explains the Debye ring patterns of the healthy tooth: we found that some peaks of points in the dentin and EDJ were merged together and the crest of the peak became blunt, but the peaks of other points in the enamel were clear and the crest of the peak was sharp. It seems that the degree of crystallinity increases on reaching the hard outer parts of the tooth, as evidenced by the higher sharpness of the diffraction lines and the lower amorphous humps.

In the carious tooth, the Debye ring patterns outside the cavity were recorded. Fig. 3(A) shows that the rings were similar to the healthy tooth enamel: they were discontinuous but distinct on the whole. However, at the point inside the cavity, Fig. 3(B) shows that the Debye rings were continuous but indefinite, the signal was weak, indicating that caries destroyed the crystal and contributed to decreased crystallinity and the disappearance of texture. The diffractogram of two points in the carious tooth in Fig. 3(C) indicates that caries destroyed the apatite crystal, producing an amorphous substance; some characteristic peaks of hydroxyapatite disappeared and merged with the high background, and, compared with the test point outside the cavity, the crystallinity of the test point inside the cavity decreased greatly.

3.2. Phase analysis

Phase analysis was carried out based on the search/match results of the *EVA* program. The main phases at point 4 of the healthy tooth were hydroxyapatite [$\text{Ca}_5(\text{PO}_4)_3(\text{OH})$, JCPDS 24-0033] and hydroxylapatite, chlorian [$\text{Ca}_5(\text{PO}_4)_3(\text{OH},\text{Cl},\text{F})$, JCPDS 25-0166]. Points 4, 5, 6 were in the enamel; their diffractograms were similar on the whole, and thus the main phases of healthy tooth enamel were the above two components.

Phase analysis of the carious tooth was also carried out. The main phases at the point outside the cavity were hydroxyapatite [$\text{Ca}_5(\text{PO}_4)_3(\text{OH})$, JCPDS 24-0033] and calcium hydrogen phosphate [CaHPO_4 , JCPDS 02-1351]. However, phase analysis was not possible at the point inside the cavity because caries had destroyed the inorganic structure of the tooth, the diffraction signal was too weak and some peaks were even lost.

3.3. Crystal size

The average crystallite size measured by the diffracting planes (211) was calculated using the Scherrer equation, $D = K\lambda/(\beta/2\cos\theta)$ (Moore & Reynolds, 1997), where D is the crystallite size in nm, K is the Scherrer constant (here $K = 0.9$), λ is the X-ray wavelength in nm, $\beta/2$ is the experimental full width at half-maximum intensity of the diffraction peak (211), and θ is the diffraction angle for diffraction peak (211). The crystallite size at different points in the healthy tooth was calculated. Fig. 4(A) shows that the average crystallite size was small at points 1, 2, 3 (approximately 10 nm), while the average crystallite size at points 4, 5, 6 was relatively large (crystallite size nearly equal to 26 nm). This suggests that average crystallite size increases from the dentin to the enamel.

3.4. Texture

Figs. 2(D), 2(E) and 2(F) show that the apatite crystal in the enamel displays a pronounced preferred orientation. We analysed the

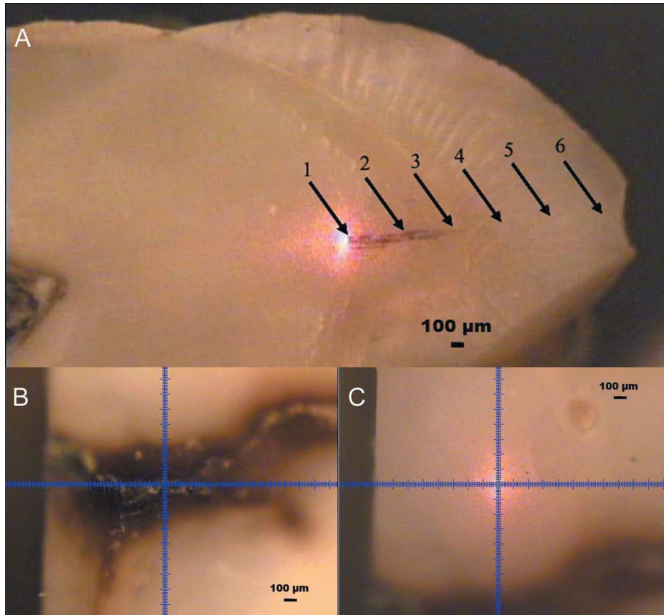


Figure 1
Analysis spots in the natural healthy tooth and the carious tooth by X-ray microdiffraction. (A) The six measurement points in the healthy tooth were determined along a line from the dentin to the enamel surface by laser pointer and microscope, the space between each was 500 μm. (B) Analysis points on the carious tooth inside the cavity, and (C) analysis points on the carious tooth outside the cavity.

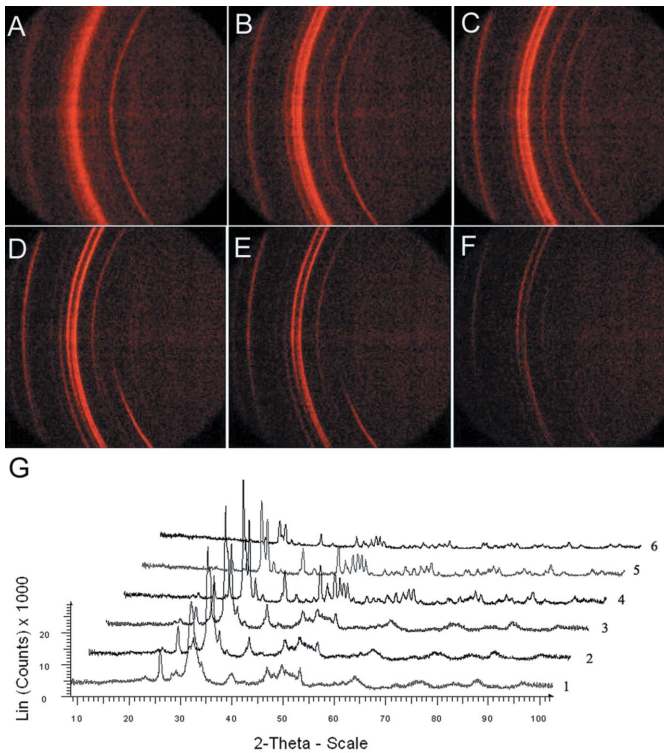


Figure 2
The X-ray microdiffraction Debye ring patterns and diffractogram of the healthy tooth. The Debye rings of positions 1, 2 and 3 in the dentin and EDJ (A, B, C) were intact and continuous. The Debye rings of positions 4, 5 and 6 in the enamel (D, E, F) were not intact and discontinuous, suggesting a texture effect or preferred orientation of these zones. (G) The X-ray microdiffractogram of the natural healthy tooth at different points: 1–6 indicate the diffractogram of points 1–6.

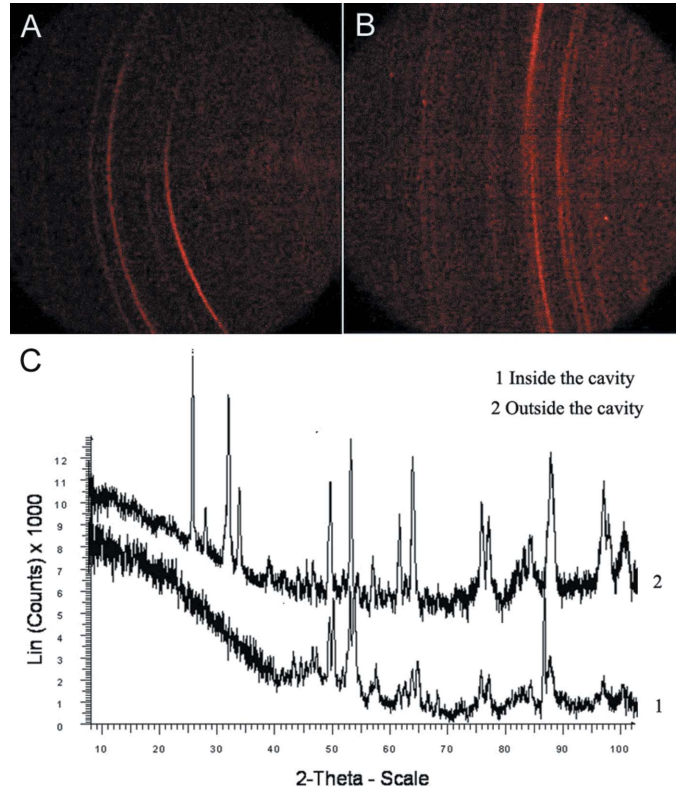


Figure 3
The X-ray microdiffraction Debye ring patterns of the carious tooth. (A) Outside the cavity the Debye rings were discontinuous but distinct on the whole. (B) Inside the cavity the Debye rings were continuous but indefinite, suggesting that the crystals were destroyed. (C) The X-ray microdiffractogram of the carious tooth. 1: inside the cavity, peaks in the interval from 10° to 40° disappeared with high background, suggesting that caries destroys the apatite crystal into an amorphous substance. 2: outside the cavity, the whole diffractogram was similar to the healthy tooth.

variation of intensity ratios for the three maximum intensity lines (211), (300) and (002). According to PDF 24-0033, for a random hydroxyapatite powder mixture, the reference intensity ratios for (211), (300), (002) are $I(211)/I(300) = 1.82$ and $I(211)/I(002) = 2.38$. To quantify the degree of texture effect, the parameter *R*, or texture index, was proposed (Low, 2004). The values of *R* for (300) and (002) were calculated according to the following equations: $R_{300} = [I(211)/I(300)]/1.82$ and $R_{002} = [I(211)/I(002)]/2.38$.

When *R* = 1.0 the apatite crystal was randomly distributed, whereas *R* values greater or lower than 1.0 indicate the presence of crystal preferred orientation or texture. Variation of *R*₃₀₀ and *R*₀₀₂ at different test points in the healthy tooth was analysed and the results are shown in Fig. 4(B). We found that for reflection (002) texture was evident at different test points, especially in the enamel, whereas there was almost no variation of texture at different test points for reflection (300). This indicated the existence of crystal preferred orientation of reflection (002).

4. Discussion

It is known that different zones in natural teeth have different composition and structure, and these different zones of teeth can be easily analysed using X-ray microdiffraction. As each substance has unique diffraction peaks, we could identify the sample diffraction peaks by comparison with standard diffraction peaks (the PDF card),

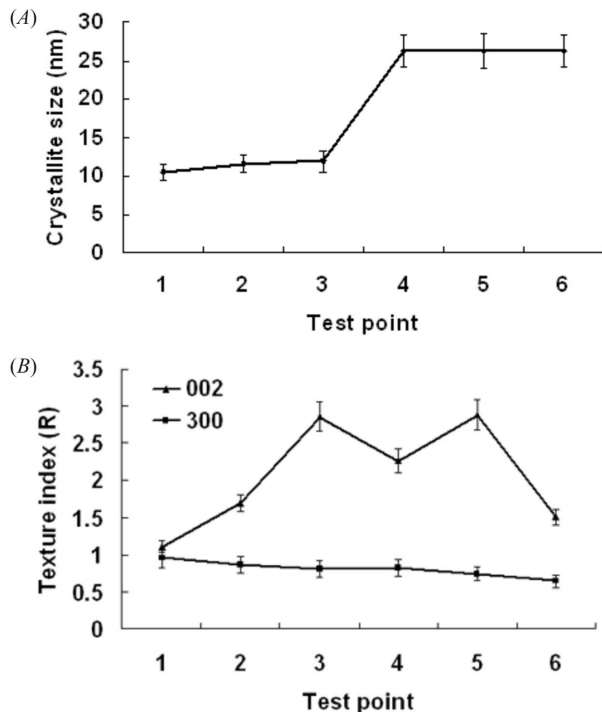


Figure 4
The crystal size and texture index of different points in the healthy tooth. (A) The crystal size of different points in the healthy tooth. (B) Variation of the texture index R , for reflections (300) and (002) at different test points in the healthy tooth.

allowing us to determine the constituent phases at different zones of the tooth. By estimating the crystal size, according to the Scherrer equation, we could calculate the average crystal size at different zones of the tooth. Also, by using the technique of microdiffraction, we could easily analyse texture or preferred crystal orientation at different zones of the tooth *in situ*, which is not possible with powder diffraction.

Our experiment showed that different zones of the natural healthy tooth from the dentin to the enamel have a different mineral composition and crystal structure; although the main component was hydroxyapatite, differences were found in different zones of the tooth. From the diffractogram and Debye ring patterns, we found that the crystallinity in the enamel was better than that in the dentin and EDJ; the average crystallite size in the enamel was larger than that in the dentin, which is similar to the results of previous studies (Gawda *et al.*, 2003; Vieira *et al.*, 2003).

The main phases of the healthy tooth enamel that we analysed were hydroxylapatite and hydroxylapatite, chlorian. Some authors have reported that natural teeth might contain fluorapatite or carbonate-apatite which may be related to the water fluoride level and the CO_2 level in the blood and tissue fluid. Hydroxyapatite, fluorapatite and carbonate-apatite are an isomorphous series of one another, the latter two substances resulting from the OH ion in hydroxyapatite being substituted by an F ion and the PO_4 ion being substituted by a CO_3 ion. The carbonate-apatite was thought to be relevant to the early stages of dental decay, as it was apparent that carbonate inclusion in apatite markedly changed its properties and increased its solubility. Fluorapatite is the most stable among the dental apatites, and has less solubility and more acid resistance than hydroxyapatite (LeGeros *et al.*, 1996; Mathew & Takagi, 2001;

LeGeros & Ming, 1983; Ten Cate, 1997; Legeros, 1991; Gruner *et al.*, 1937).

The texture effect of the natural tooth was discovered many years ago; it was also called 'two fiber axes', and was thought to exist in the Hunter-Schreger bands in the enamel (Bergman & Lind, 1966; Hirota, 1982, 1986). In our experiment we observed an obvious texture effect in the enamel with the Debye ring patterns; further calculation of the texture index revealed that the crystal preferred orientation was mainly evident in the reflection (002), which is similar to the findings of Hirota (1986) who considered that the phenomenon was caused by the reflections of two zones of the Hunter-Schreger bands being recorded simultaneously on X-ray film.

According to our analysis, it is clear that the X-ray diffractogram and Debye ring patterns at different zones of the tooth are not the same; the differences found include varied crystallinity and component phases and crystal preferred orientation. Using this technique of fast online measurements by high-resolution X-ray microdiffraction, it should be possible to obtain more detailed information on, for example, layer orientation and continued decay variation in tooth apatite crystal. Combining the X-ray microdiffraction technique with other analytical instruments such as Fourier transform infrared spectroscopy and scanning electron microscopy would help to provide valuable information on the variation and mechanism of tooth development and the effects of decay.

The sample data were collected at Bruker AXS in Germany, and we would like to acknowledge Bruker's support for this study.

References

- Bergman, G. & Lind, P. O. (1966). *J. Dent. Res.* **45**, 1477-1484.
 Busson, B., Engström, P. & Doucet, J. (1999). *J. Synchrotron Rad.* **6**, 1021-1030.
 Featherstone, J. D., Duncan, J. F. & Cutress, T. W. (1978). *Arch. Oral Biol.* **23**, 405-413.
 Friedel, F., Winkler, U., Holtz, B., Seyrich, R. & Ullrich, H. J. (2005). *Cryst. Res. Technol.* **40**, 182-187.
 Gawda, H., Sekowski, L. & Trebacz, H. (2003). *Proceedings of the World Congress on Ultrasonics*, pp. 1179-1182.
 Gross, R. (1926). Die kristalline struktur von dentin und zahnschmelz festchr. D. Zahn rztl. Inst Greifswald (Berlin), pp. 59-69.
 Gruner, J. W., McConnell, D. & Armstrong, W. D. (1937). *J. Biol. Chem.* **121**, 771-781.
 Hirota, F. (1982). *Arch. Oral Biol.* **27**, 931-937.
 Hirota, F. (1986). *J. Dent. Res.* **65**, 978-981.
 LeGeros, R. Z. (1981). *Prog. Crystal Growth Charact.* **4**, 1-45.
 LeGeros, R. Z. (1990). *J. Dent. Res.* **69** (Spec. Iss.), 567-574.
 LeGeros, R. Z. (1991). *Monographs in Oral Science*, 1st ed., pp. 108-128. Basel: Karger.
 LeGeros, R. Z. (1999). *J. Clin. Dent.* **10**, 65-73.
 LeGeros, R. Z. & Ming, S. (1983). *Caries Res.* **17**, 419-429.
 LeGeros, R. Z., Sakae, T., Bautista, C., Retino, M. & LeGeros, J. P. (1996). *Adv. Dent. Res.* **10**, 225-231.
 Low, I. M. (2004). *J. Am. Ceram. Soc.* **87**, 2125-2131.
 Mathew, M. & Takagi, S. (2001). *J. Res. Natl. Inst. Stand. Technol.* **106**, 1035-1044.
 Moore, D. M. & Reynolds, R. C. (1997). *X-ray Diffraction and the Identification and Analysis of Clay Minerals*, 2nd ed., p. 87. Oxford University Press.
 Nakano, T., Kaibara, K., Tabata, Y., Nagata, N., Enomoto, S., Marukawa, E. & Umakoshi, Y. (2002). *Bone*, **31**, 479-487.
 Robinson, C., Shore, R. C., Brookes, S. J., Strafford, S., Wood, S. R. & Kirkham, J. (2000). *Crit. Rev. Oral Biol. Med.* **11**, 481-495.
 Ten Cate, J. M. (1997). *Eur. J. Oral Sci.* **105**, 461-465.
 Vieira, A., Hancock, R., Limeback, H., Schwartz, M. & Grynypas, M. (2003). *J. Dent. Res.* **82**, 909-913.